

Solid-phase C₆₀ in the peculiar binary XX Oph?

A. Evans,^{1*} J. Th. van Loon,¹ C. E. Woodward,² R. D. Gehrz,² G. C. Clayton,³
L. A. Helton,^{2,4} M. T. Rushton,⁵ S. P. S. Eyres,⁵ J. Krautter,⁶ S. Starrfield⁷
and R. M. Wagner⁸

¹*Astrophysics Group, Keele University, Keele, Staffordshire ST5 5BG*

²*Minnesota Institute for Astrophysics, School of Physics & Astronomy, 116 Church Street SE, University of Minnesota, Minneapolis, MN 55455, USA*

³*Department of Physics and Astronomy, Louisiana State University, Baton Rouge, LA 70803, USA*

⁴*Stratospheric Observatory for Infrared Astronomy, NASA Ames Research Center, MS 211-3, Moffett Field, CA 94035, USA*

⁵*Jeremiah Horrocks Institute, University of Central Lancashire, Preston PR1 2HE*

⁶*Landessternwarte, Zentrum für Astronomie der Universität Heidelberg, Koenigstuhl, D-69117 Heidelberg, Germany*

⁷*School of Earth and Space Exploration, Arizona State University, PO Box 871404, Tempe, AZ 85287-1404, USA*

⁸*Large Binocular Telescope Observatory, 933 North Cherry Avenue, Tucson, AZ 85721, USA*

Accepted 2011 December 22. Received 2011 December 7; in original form 2011 June 23

ABSTRACT

We present infrared spectra of the binary XX Oph obtained with the Infrared Spectrograph on the *Spitzer Space Telescope*. The data show some evidence for the presence of solid C₆₀ – the first detection of C₆₀ in the solid phase – together with the well-known ‘unidentified infrared’ emission features. We suggest that, in the case of XX Oph, the C₆₀ is located close to the hot component, and that in general it is preferentially excited by stars having effective temperatures in the range 15 000–30 000 K. C₆₀ may be common in circumstellar environments, but unnoticed in the absence of a suitable exciting source.

Key words: astrochemistry – binaries: symbiotic – circumstellar matter – stars: individual: XX Oph – infrared: stars.

1 INTRODUCTION

The possible existence of buckminsterfullerene (C₆₀) in astrophysical environments has long been suggested (Kroto & Jura 1992), but only recently has observational evidence for emission from C₆₀ in the gas phase been forthcoming. Gas phase C₆₀ has now been detected in the environments of young planetary nebulae (Cami et al. 2010; Zhang & Kwok 2011), RCB stars (García-Hernández, Kameswara Rao & Lambert 2011) and in the reflection nebulae NGC 2023 and NGC 7023 that are illuminated by B stars (Sellgren et al. 2010). In the case of the low-excitation planetary nebula Tc 1, Cami et al. (2010) argue that the C₆₀ (and C₇₀) molecules are attached to the surfaces of cooler carbonaceous grains. Many of the objects displaying C₆₀ also have strong ‘unidentified infrared’ (UIR) features.

The formation of C₆₀ and other fullerenes in terrestrial laboratories usually requires a hydrogen-deficient environment, and this seems to be consistent with their presence in the environments of (evolved) H-deficient carbon stars (Cami et al. 2010; García-Hernández et al. 2011). However, the detection of C₆₀ in the reflection nebulae NGC 2023 and NGC 7023 (Sellgren et al. 2010) indicates that fullerene formation is possible in young (H-rich)

environments. UIR features, as well as ‘extended red emission’ attributed, among other hypotheses, to small – possibly ionized – hydrocarbon molecules, are seen in the environment of NGC 7023 (Berné et al. 2008; Sellgren et al. 2010).

We report here the possible detection of solid phase C₆₀, in the environment of the peculiar binary XX Oph, observed with the *Spitzer Space Telescope* (Werner et al. 2004a; Gehrz et al. 2007).

2 THE XX OPH BINARY

XX Oph is a binary consisting of a late (M7III) giant and an early (B0V?) star (see e.g. de Winter & Thé 1990; Evans et al. 1993 and references therein; Cool et al. 2005 give M6-8II). It is sometimes classed as a Be star (e.g. de Winter & Thé 1990) and sometimes as a symbiotic (Samus et al. 2011). However, it shows few of the common symptoms of symbiosis, such as the presence of high excitation emission lines.

While there is photometric and spectroscopic evidence that a cool component in the XX Oph system dominates in the red (de Winter & Thé 1990; Evans et al. 1993; Cool et al. 2005), understanding the nature of the hot component has proven to be problematic. The evidence is circumstantial: there is spectroscopic evidence for a ‘hot companion’ in the blue, in the form of H (and other) emission lines.

Lockwood, Dyck & Ridgway (1975) argued that XX Oph is heavily reddened and estimated the extinction, A_v, to be ~4 mag.

*E-mail: ae@astro.keele.ac.uk

Spectrophotometry of XX Oph was presented by Blair et al. (1983), who deduced $E(B - V) \simeq 1.08$ mag on the basis of the $H\alpha/H\beta$ ratio. They noted that this is significantly less than the value given by Lockwood et al., unless the ratio of total-to-selective extinction is $R \simeq 3.7$, but the polarization of XX Oph is inconsistent with a high value of R (Evans et al. 1993).

Although a B0V? classification is assigned to the hot component, the presence of a massive ($\sim 20 M_{\odot}$) star in the XX Oph system seems unlikely on kinematic grounds. For a distance of ~ 2 kpc (Evans et al. 1993) it lies ~ 400 pc above the Galactic plane and its proper motion (Hipparcos 1997) takes it towards the plane – highly unlikely for a B0V? star.

Furthermore, the spectral energy distribution – from 4400 \AA to $100 \mu\text{m}$ – can be fitted (bearing in mind the variability) by a two-component DUSTY (Ivezić & Elitzur 1995) model. The hot component is a B *subdwarf* at the centre of a dust shell having $0.01 \mu\text{m}$ amorphous carbon grains with a temperature of 800 K at the inner boundary and an optical depth of ~ 0.001 in the visual. The cool component is a M7III star that effectively plays no part in heating the dust (see Fig. 1). The DUSTY fit assumes that the dust shell is spherically symmetric with the B star located at its centre, so clearly the fit has its limitations (e.g. a disc is more likely in a binary). However, the inner boundary of the dust shell is $\sim 7.2 \times 10^{11} \text{ m}$ from the B star. The size of the Strömgren sphere associated with the B star exceeds this if the gas density in its vicinity $\lesssim 10^{13} \text{ m}^{-3}$.

The reclassification of the hot component as a subdwarf removes the need for the large reddening assigned by Lockwood et al. and others, and is consistent with an interstellar reddening $E(B - V) = 0.51$ mag (Evans et al. 1993). It also has implications for the nature and evolution of the binary.

Although the cool component in XX Oph seems to be oxygen-rich – as evidenced by the presence of TiO and VO bands – the 8.6- and $11.2\text{-}\mu\text{m}$ UIR features reported in the IR spectrum of XX Oph by Evans (1994) are typical of carbon-rich environments. However, the usual 3.28- and $3.4\text{-}\mu\text{m}$ UIR features are weak.

Fig. 2 shows a spectrum of XX Oph obtained with the Short Wavelength Spectrometer (SWS; de Graauw et al. 1996) on the *Infrared Space Observatory* (Kessler et al. 1996) that confirms the

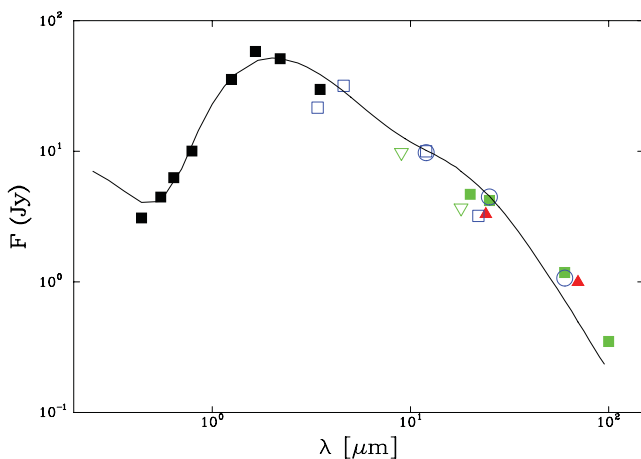


Figure 1. Photometry of XX Oph, dereddened for $E(B - V) = 0.51$ (Evans et al. 1993). Filled black squares – *BVRI JHKL* (Evans et al. 1993); open blue squares – *WISE* (Wright et al. 2010); inverted green triangles – *AKARI* (Murakami et al. 2007); open blue circles – *IRAS PSC*; filled green squares – *ISO PHOT-P*; red triangles – *Spitzer Space Telescope MIPS*. In all cases, errors are smaller than the plotted points. Curve is DUSTY fit with parameters given in text; see text for details.

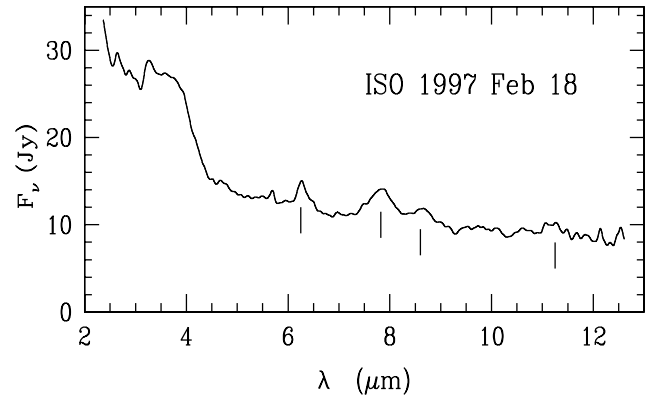


Figure 2. *ISO SWS* spectrum of XX Oph; the 6.25- , 7.7- , 8.6- and $11.2\text{-}\mu\text{m}$ UIR features are identified. The apparent peak at $3.3 \mu\text{m}$ may be due to the $3.3\text{-}\mu\text{m}$ UIR feature, but the spectrum in this region is dominated by molecular absorption in the M giant.

UIR features at 8.6 and $11.2 \mu\text{m}$ reported by Evans (1994). The UIR feature at $6.25 \mu\text{m}$ is detected and the non-detection of the 3.28- and $3.4\text{-}\mu\text{m}$ UIR features is confirmed. The ‘ $8\text{-}\mu\text{m}$ ’ feature reported by Evans is the long wavelength wing of the well-known ‘ $7.7\text{-}\mu\text{m}$ ’ feature, affected by inadequate cancellation of the atmosphere near the edge of the $8\text{--}13 \mu\text{m}$ window.

In most stars, the flux in the $3.28\text{-}\mu\text{m}$ UIR feature is typically comparable to that of the ‘ 7.7 ’ feature (e.g. Tielens 2008). On this basis we would expect the $3.28\text{-}\mu\text{m}$ feature in XX Oph to have a peak flux $\sim 3 \text{ Jy}$. While there is indeed evidence for a feature at $\sim 3.3 \mu\text{m}$ (see Fig. 2), the spectrum in this region is dominated by molecular absorption (e.g. CO, OH) in the M giant, which has a flux of $\sim 32 \text{ Jy}$ at $3 \mu\text{m}$. The apparent absence of the $3.28\text{-}\mu\text{m}$ feature can presumably be attributed to the fact that it is swamped by the emission from the M star.

The variability of XX Oph is irregular, although the Hipparcos catalogue (Hipparcos 1997) lists it as having a possible period of 3.52 d , and as displaying sudden dips in luminosity. Sobotka (2004) reported that XX Oph went into a deep (eclipse-like) minimum in 2005, the first in 37 years (see Fig. 3). Cool et al. (2005) found that the equivalent width of $H\alpha$ increased during the minimum, indicating that the continuum around 656 nm had faded.

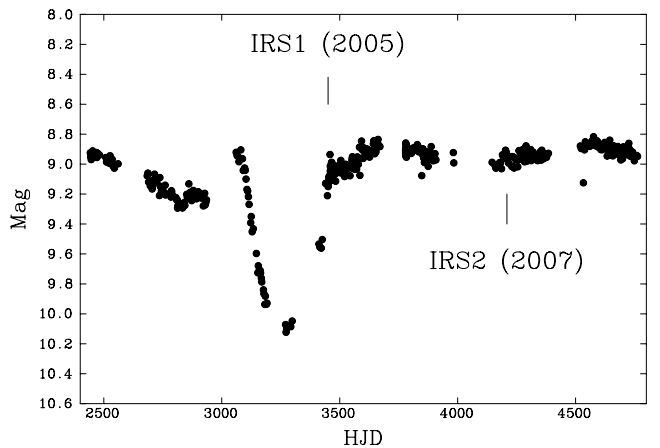


Figure 3. The V-band light curve of XX Oph from the All Sky Automated Survey (ASAS) data base (Pojmański 2002). The times of the *Spitzer Space Telescope IRS* observations are indicated.

We note that, with a B subdwarf, most of the *V*-band light from the XX Oph system comes from the M star, so that the eclipse in Fig. 3 must be of the giant, presumably by material in the vicinity of the B star. The optical depth at *V* at eclipse minimum is $\tau_V \approx 1.0$, far greater than that required for the IR excess in Fig. 1, underlining the fact that the *DUSTY* fit should not be taken too literally.

3 OBSERVATIONS

XX Oph was observed with the *Spitzer* Infrared Spectrograph (IRS; Houck et al. 2004) in staring mode on two occasions as XX Oph was emerging from a deep minimum and some 2 years thereafter. The blue peak-up array was used to centre the object in the IRS slits. Observations were also obtained with the Multi-band Imaging Photometer (MIPS) for *Spitzer* (Rieke et al. 2004). Spectra were obtained with both low- and high-resolution IRS modes, covering the spectral range of 5–38 μm . For the high-resolution modes, we also obtained observations of the background; however, as we are comparing data from two epochs, the background measurement is not critical. The spectrum was extracted from the version 12.3 processed pipeline data product using *SPICE* version 2.2 (Spice 2005).

The spectra for the two epochs are shown in Fig. 4. There may be some evidence for the 18- μm silicate feature, but the corresponding 9.7- μm feature is very weak. However, the UIR features are clearly present, as is an excess longwards of $\sim 15 \mu\text{m}$ due to emission by circumstellar dust (cf. Fig. 1). Such ‘chemical dichotomy’ (i.e. environments with a mix of C-rich and O-rich dust) is of course not uncommon (e.g. Clayton et al. 2011, and references therein).

There has clearly been a change in the IR spectrum between 2005 and 2007. In particular, H recombination lines are present in 2005 (as XX Oph was emerging from eclipse) but were apparently weak in 2007; for example, the flux in $\text{H}\alpha$ 12.371 μm was 1.61

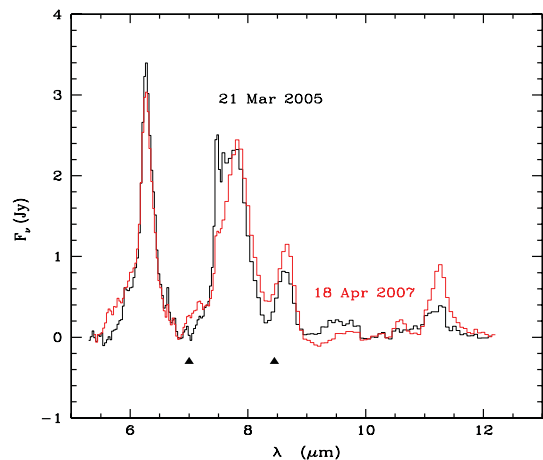


Figure 5. UIR features in XX Oph; the expected wavelengths of the C_{60} features are indicated by the triangles. The apparent ‘excess’ at $\sim 7.5 \mu\text{m}$ in the ‘7.7’ UIR feature in 2005 is due to the presence of $\text{H}1$ 6–5 and 8–6. The flux uncertainties in this wavelength range are typically $\pm 0.03 \text{ Jy}$.

$[\pm 0.05] \times 10^{-15} \text{ W m}^{-2}$ in 2005, compared with $5.5 [\pm 1] \times 10^{-16} \text{ W m}^{-2}$ in 2007. However, both $\text{H}\alpha$ and $\text{H}\beta$ are present in an optical spectrum of XX Oph obtained on 2007 May 8 (within days of the 2007 IRS spectrum) by one of us (LAH), as are a number of ‘diffuse interstellar bands’, which most likely are of interstellar origin. These data will be presented in a future paper (Helton et al., in preparation).

We have extracted a continuum from both spectra to highlight the UIR features; the result is shown in Fig. 5. There was little change between 2005 and 2007, except that the 11.3 and 8.6- μm UIR

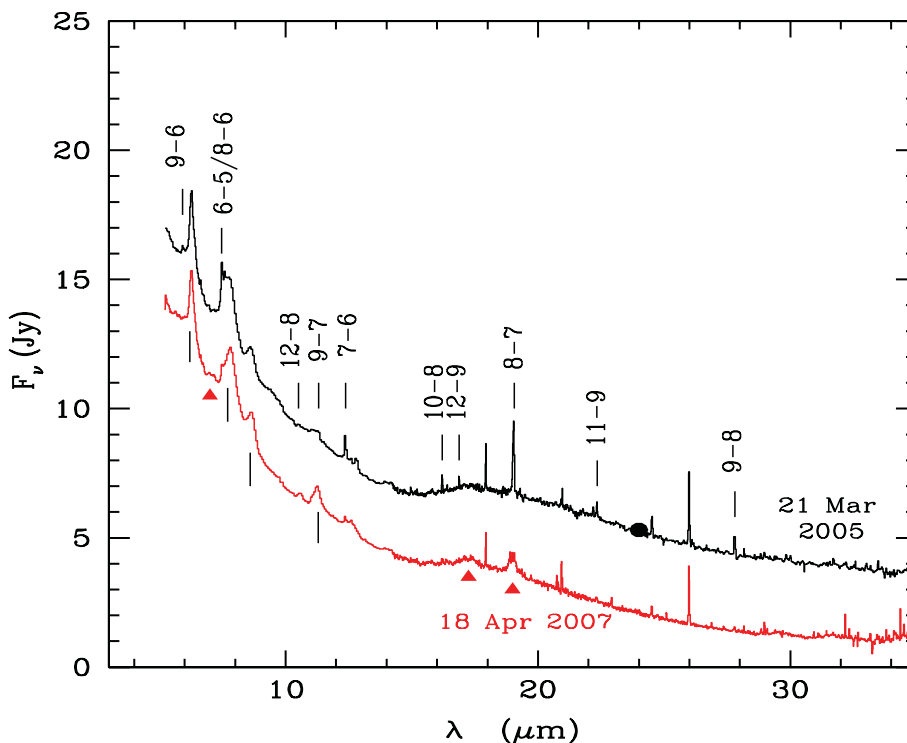


Figure 4. *Spitzer* Space Telescope IRS spectrum of XX Oph in 2005 and 2007; the 2005 data have been displaced upwards by 2 Jy for clarity. The 6.25-, 7.7-, 8.6- and 11.2- μm UIR and H recombination lines are identified; note the absence of H recombination lines in 2007. The point at 24 μm is the MIPS photometry. The possible C_{60} features at 7.1, 17.25 and 19 μm in the 2007 data are indicated by triangles; see also Fig. 6 below.

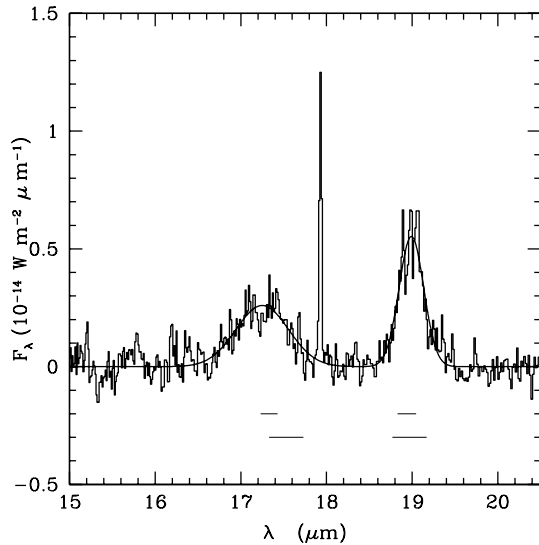


Figure 6. Possible *C*₆₀ features in XX Oph. The upper horizontal lines indicate the wavelengths of the ‘17.3-’ and ‘18.9- μm ’ features in *C*₆₀ smoke (Krätschmer et al. 1990a), the lower lines of the corresponding features in gaseous *C*₆₀ (Frum et al. 1991).

features were significantly stronger in 2007 (when the IR hydrogen emission lines were weak).

The central wavelengths of the UIR features in XX Oph (e.g. $7.48 \pm 0.01 \mu\text{m}$ in 2005, $7.79 \pm 0.01 \mu\text{m}$ in 2007 for the ‘7.7’ feature) are consistent with excitation by a source with an effective temperature in excess of $\sim 10^4 \text{ K}$ (e.g. Sloan et al. 2007; Acke 2011), and therefore with excitation by the B star. The changes we see in the strengths and possibly central wavelengths of the UIR features may be associated with changes in the ionization of the polycyclic aromatic hydrocarbon (PAH; e.g. Draine & Li 2001), possibly as a result of changes in the extinction in the dust shell around the B star.

Fig. 4 also shows clear evidence for two broad features that are present in 2007 but not in 2005. We have subtracted the continuum to highlight these features (see Fig. 6). Features at these wavelengths are included in the PAHFIT package (Smith et al. 2007), but we consider it unlikely that the two features in XX Oph are due to emission by PAH molecules, for the following reasons: (i) their absence in 2005, when other UIR features were present; (ii) the strength of the 19- μm feature compared with that of the 17.4 μm ; (iii) the 17.4/7.7 μm flux ratio. The 17.4- μm feature was reported in NGC 7023 by Werner et al. (2004b), who assigned it to ‘aromatic hydrocarbons or nanoparticles of unknown mineralogy’; it has subsequently been attributed to *C*₆₀ (Sellgren et al. 2010).

Possible identifications for these features are 17.4 and 18.9 μm *C*₆₀, which in the gas phase has four active vibrational modes, at $\sim 7.0, 8.5, 17.5$ and $18.9 \mu\text{m}$ (e.g. Frum et al. 1991). Fig. 4 also

shows evidence for a feature at $\sim 7 \mu\text{m}$, and subtraction of the 2005 spectrum from the 2007 spectrum leaves a feature with central wavelength $7.01 \pm 0.01 \mu\text{m}$ (see Table 1); there is no evidence for the ‘8.5- μm ’ feature.

The ‘17.4- μm ’ feature we observe in XX Oph is actually at 17.25 μm , quite different from the expected value of 17.53 μm for gas phase *C*₆₀ (Frum et al. 1991). However, *solid* *C*₆₀ has a feature at 17.3 μm (Krätschmer, Fostropoulos & Huffman 1990a; Krätschmer et al. 1990b), closer to the 17.25- μm feature in XX Oph. We should therefore consider whether the features in Fig. 6 arise in gaseous or solid *C*₆₀.

The flux ratios of the putative *C*₆₀ features enable an estimate of the vibrational temperature T_{vib} if the *C*₆₀ is in gaseous form. Using Einstein coefficients from Mitzner & Campbell (1995; included in Table 1), values of $T_{\text{vib}} \sim 520 \pm 50 \text{ K}$ are obtained; however, the ‘18.9- μm ’ flux seems underestimated by a factor ~ 2 . A similar value ($\sim 670 \text{ K}$) is obtained assuming that the energy of a $\sim 10 \text{ eV}$ photon absorbed by a *C*₆₀ molecule is equally distributed amongst the available vibrational modes. However, at this temperature, the ‘8.5- μm ’ feature would have a flux $\sim 1.5 \times 10^{-15} \text{ W m}^{-2}$, far greater than observed. We also note that laboratory measurements on solid *C*₆₀ (Krätschmer et al. 1990a) suggest that the ‘8.5- μm ’ feature is rather weaker than the other three. Therefore, on the basis of (i) the wavelength of the ‘17.4- μm ’ feature and (ii) the weakness of the ‘8.5- μm ’ feature, we conclude that the *C*₆₀ in XX Oph is most likely in solid form; if so, this is the first astrophysical detection of solid *C*₆₀.

The absorption cross-section of *C*₆₀ has been measured by Yagi et al. (2009), from which we estimate the Planck mean absorption cross-section per *C*₆₀ molecule (averaged over the emission of the B star) to be $\sim 7 \times 10^{-21} \text{ m}^2$. If (cf. Section 2) the B star is situated at $\sim 7.2 \times 10^{11} \text{ m}$ from the inner boundary of the dust shell, the temperature of a *C*₆₀ grain of radius a is $\sim 200 (a/0.03 \mu\text{m})^{1/4} \text{ K}$.

While the apparent absence of *C*₆₀ in the IRS spectrum immediately after eclipse in 2005, and its presence in 2007, is suggestive, it is difficult to argue that the eclipse is in any way connected with the presence of *C*₆₀ in the spectrum, especially as it is the giant that is eclipsed: it is likely therefore that the appearance of *C*₆₀ in 2007 is unconnected with the eclipse of Fig. 3.

4 C₆₀ IN XX OPH

We can make an estimate of the mass of *C*₆₀ using the combined flux in the *C*₆₀ features. Assuming (cf. Section 2) the B star is situated at $\sim 7.2 \times 10^{11} \text{ m}$ from the inner boundary of the dust shell, and using the Planck mean absorption cross-section above, the absorbed power per *C*₆₀ particle is $\sim 8.1 \times 10^{-18} \text{ W}$. The emitted power (assuming a distance of 2 kpc for XX Oph; Evans et al. 1993) is $\sim 3.9 \times 10^{26} \text{ W}$, so $\sim 4.8 \times 10^{43}$ *C*₆₀ particles (i.e. $\sim 2.9 \times 10^{-11} M_{\odot}$), in solid form, are required. This suggests that the number of *C*₆₀ molecules is ~ 0.03 the number of PAH molecules.

Table 1. Properties of *C*₆₀ features in XX Oph; wavelengths of gaseous and solid *C*₆₀ features from Frum et al. (1991) and Krätschmer et al. (1990a), respectively. Einstein coefficients A from Mitzner & Campbell (1995).

| λ (μm) | FWHM (μm) | Flux ($10^{-15} \text{ W m}^{-2}$) | Gas λ (μm) | Solid λ (μm) | A (s^{-1}) |
|-----------------------------|------------------------|--------------------------------------|---------------------------------|-----------------------------------|-------------------------|
| 7.01 ± 0.01 | 0.25 ± 0.01 | 4.1 ± 0.2 | 7.11 | 7.00 | 151.6 |
| 8.5 | | <0.2 | 8.55 | 8.45 | 74.8 |
| 17.25 ± 0.02 | 0.72 ± 0.04 | 2.00 ± 0.10 | 17.53 | 17.33 | 14.6 |
| 18.99 ± 0.01 | 0.34 ± 0.01 | 2.00 ± 0.10 | 18.97 | 18.94 | 36.8 |

The detection of C_{60} in a range of environments (Cami et al. 2010; Sellgren et al. 2010; García-Hernández et al. 2011), including both H-poor and H-rich environments, indicates that C_{60} can form in a variety of astrophysical conditions. García-Hernández et al. suggest that both the UIR carrier and C_{60} may form as a result of the disintegration of hydrogenous amorphous carbon (HAC) grains. However, the fact that HAC is seen in environments (e.g. novae; cf. Evans et al. 2010) in which C_{60} is *not* seen indicates that there are other factors that determine whether or not C_{60} is detected.

Most of the objects in which C_{60} has been reported are associated with stars having effective temperature T_{eff} in the range $\sim 15\,000$ – $30\,000$ K, the exception being the RCB star V854 Cen ($T_{\text{eff}} \simeq 6\,750$ K). XX Oph is in the former category, while classical novae have $T_{\text{eff}} \gtrsim 50\,000$ K at the time of dust formation. Notwithstanding the small number of objects in which C_{60} has been detected, the data thus far may point to the fact that it is the effective temperature of the central star that is the common factor in the detection of C_{60} , the critical range being $\sim 10\,000$ – $30\,000$ K.

In 2007 the C_{60} in XX Oph seems to be present when the IR H recombination lines are weak, and the 8.5- and 11.2- μm UIR features are strong. This suggests either (i) that the C_{60} is not a permanent feature of the XX Oph environment but is formed when conditions are favourable (either by fragmentation of larger particles or by chemical routes from smaller molecules) or (ii) that C_{60} is a permanent feature and that its excitation is intermittent.

One possible scenario is that the C_{60} -bearing material is, as already discussed, confined to the vicinity of the B star. The H lines arise from a shell, also associated with the B star and possibly accreted from the giant wind; the relative sizes of the ionized and dusty regions depend on the gas density. The formation of C-rich dust would require the photodissociation of wind CO by UV radiation from the B star to release C for carbon chemistry (Evans 1994). Enhanced formation of C_{60} (coincidentally after the 2005 eclipse) would be consistent with the appearance of C_{60} in 2007. Quenching of the UV radiation from the B star by the C_{60} -containing dust would lead to reduced excitation of H in the shell. If this is correct, then it is likely that C_{60} is formed ‘bottom-up’ rather than ‘top-down’.

5 CONCLUSIONS

We have reported the possible detection of solid-phase C_{60} in the environment of the peculiar binary XX Oph. Contrary to previous work, we conclude that the hot star is a B subdwarf that is surrounded by an ionized shell and a C_{60} -bearing shell, most likely in the form of a disc. Variations in the optical depth of the latter result in variations in the excitation of H lines.

We will present a detailed discussion of the XX Oph system and its environment in a forthcoming paper.

ACKNOWLEDGMENTS

We thank Dr L. d’Hendecourt for helpful comments on an earlier version.

This work is based on observations made with the *Spitzer Space Telescope*, which is operated by the Jet Propulsion Laboratory, California Institute of Technology under a contract with NASA. This publication makes use of data products from the *Wide-field Infrared Survey Explorer*, which is a joint project of the University of California, Los Angeles, and the Jet Propulsion Laboratory

/California Institute of Technology, funded by the National Aeronautics and Space Administration. Based on observations with *AKARI*, a JAXA project with the participation of ESA. RDG, CEW and LAH were supported by various NASA *Spitzer*/JPL contracts and the United States Air Force. SS was supported by NASA and the NSF.

REFERENCES

- Acke B., 2011, in Joblin C., Tielens A. G. G. M., eds, EAS Publ. Ser. Vol. 46, PAHs and the Universe. Cambridge Univ Press, Cambridge, p. 259
- Berné O., Joblin C., Rapacioli M., Thomas J., Cuillandre J.-C., Deville Y., 2008, *A&A*, 479, L41
- Blair W. P., Feibelman W. A., Michalitsianos A. G., Stencel R. E., 1983, *ApJS*, 53, 573
- Cami J., Bernard-Salas J., Peeters E., Malek S. E., 2010, *Sci*, 329, 1180
- Clayton G. C. et al., 2011, *AJ*, 142, 54
- Cool R. J., Howell S. B., Peña M., Adamson A. J., Thompson R. R., 2005, *PASP*, 117, 462
- de Graauw Th. et al., 1996, *A&A*, 315, L49
- de Winter D., Thé P. S., 1990, *Ap&SS*, 166, 99
- Draine B. T., Li A., 2001, *ApJ*, 551, 807
- Evans A., 1994, *A&A*, 288, L37
- Evans A. et al., 1993, *A&A*, 267, 161
- Evans A. et al., 2010, *MNRAS*, 406, L85
- Frum C. I., Engelman R., Hedderich H. G., Bernath P. F., Lamb L. D., Huffman D. R., 1991, *Chem. Phys. Lett.*, 176, 504
- García-Hernández D. A., Kameswara Rao N., Lambert D. L., 2010, *ApJ*, 729, 126
- Gehr R. D. et al., 2007, *Rev. Sci. Instr.*, 78, 011302
- Hipparcos, 1997, The Hipparcos Catalogue, The European Space Agency, ESA Publ. SP-1200
- Houck J. R. et al., 2004, *ApJS*, 154, 18
- Ivezić Ž., Elitzur M., 1995, *ApJ*, 445, 415
- Kessler M. et al., 1996, *A&A*, 315, L27
- Krätschmer W., Fostiropoulos K., Huffman D. R., 1990a, *Chem. Phys. Lett.*, 170, 167
- Krätschmer W., Lamb L. D., Fostiropoulos K., Huffman D. R., 1990b, *Nat*, 347, 354
- Kroto H. W., Jura M., 1992, *A&A*, 263, 275
- Lockwood G. W., Dyck H. M., Ridgway S. T., 1975, *ApJ*, 195, 385
- Mitzner R., Campbell E. E. B., 1995, *J. Chem. Phys.*, 103, 2445
- Murakami H. et al., 2007, *PASJ*, 59, S369
- Pojmanski G., 2002, *Acta Astron.*, 52, 397
- Reike G. H. et al., 2004, *ApJS*, 154, 25
- Samus N. N. et al., 2011, General Catalog of Variable Stars (GCVS database, version of 2011 Jan)
- Sellgren K., Werner M. W., Ingalls J. G., Smith J. D. T., Carelton T. M., Joblin C., 2010, *ApJ*, 722, L54
- Sloan G. C. et al., 2007, *ApJ*, 664, 1144
- Smith J. D. T. et al., 2007, *ApJ*, 656, 770
- Sobotka P., 2004, *Inf. Bull. Var. Stars*, 5571, 1
- Spice, 2005, Spice User’s Guide, Version 1.1 (<http://ssc.spitzer.caltech.edu/postbcd/spice.html>)
- Tielens A. G. G. M., 2008, *ARA&A*, 46, 289
- Werner M. W. et al., 2004a, *ApJS*, 154, 1
- Werner M. W., Uchida K. I., Sellgren K., Marengo M., Gordon K. D., Morris P. W., Houck J. R., Stansberry J. A., 2004b, *ApJS*, 154, 309
- Wright E. L. et al., 2010, *AJ*, 140, 1868
- Yagi H. et al., 2009, *Carbon*, 47, 1152
- Zhang Y., Kwok S., 2011, *ApJ*, 730, 126

This paper has been typeset from a $\text{\TeX}/\text{\LaTeX}$ file prepared by the author.